

PDF hosted at the Radboud Repository of the Radboud University Nijmegen

The following full text is a publisher's version.

For additional information about this publication click this link.

<http://hdl.handle.net/2066/26898>

Please be advised that this information was generated on 2017-12-05 and may be subject to change.

Neutral strange particle production in K^+ and π^+ collisions with Al and Au nuclei at 250 GeV/c

EHS-NA22 Collaboration

F. Botterweck^a, M. Charlet^{a,1}, P.V. Chliapnikov^b, A. De Roeck^{c,2}, E.A. De Wolf^{c,3}, K. Dziunikowska^d, P.E. Ermolov^e, A. Eskreys^d, Z.C. Garutchava^f, G. Gulkanyan^g, R.Sh. Hakobyan^g, T. Haupt^{a,4}, K. Kaleba^d, W. Kittel^a, D. Kisielewska^d, A.B. Michalowska^c, V.I. Nikolaenko^b, K. Olkiewicz^d, V.M. Ronjin^b, A.G. Tomaradze^f, F. Verbeure^c, R. Wischnowski^h, S.A. Zotkin^e

^a University of Nijmegen and NIKHEF-H, NL-6525 ED Nijmegen, The Netherlands

^b Institute for High Energy Physics, SU-142284 Serpukhov, USSR

^c Dept. of Physics, Universitaire Instelling Antwerpen, B-2610 Wilrijk, and Interuniversity Institute for High Energies, B-1050 Brussels, Belgium

^d Institute of Physics and Nuclear Techniques of the Academy of Mining and Metallurgy and Institute of Nuclear Physics, PL-30055 Krakow, Poland*

^e Moscow State University, SU-119899 Moscow, USSR

^f Institute of High Energy Physics, Tbilisi State University, SU-380086 Tbilisi, USSR

^g Institute of Physics, SU-375036 Yerevan, USSR

^h Institut für Hochenergiephysik, O-1615 Berlin-Zeuthen, Federal Republic of Germany

Received 6 February 1992; revised form 24 May 1992

Abstract. Data are presented on inclusive K_S^0 and Λ production in K^+ and π^+ collisions with Al and Au nuclei at 250 GeV/c. Results are given on total inclusive cross sections and their A dependence, as well as on distributions in Feynman- x_F , rapidity y and transverse momentum. Ratios of K_S^0 and of Λ to π^- production are presented. The data are compared with predictions of the quark-parton model FRITIOF.

$$K^+ \text{ Al} \rightarrow \Lambda + X, \quad (5)$$

$$K^+ \text{ Au} \rightarrow \Lambda + X, \quad (6)$$

$$\pi^+ \text{ Al} \rightarrow \Lambda + X, \quad (7)$$

$$\pi^+ \text{ Au} \rightarrow \Lambda + X, \quad (8)$$

$$K^+ \text{ Al} \rightarrow \bar{\Lambda} + X, \quad (9)$$

$$K^+ \text{ Au} \rightarrow \bar{\Lambda} + X, \quad (10)$$

$$\pi^+ \text{ Al} \rightarrow \bar{\Lambda} + X, \quad (11)$$

$$\pi^+ \text{ Au} \rightarrow \bar{\Lambda} + X. \quad (12)$$

1 Introduction

In this paper we report on a study of inclusive production of K_S^0 , Λ and $\bar{\Lambda}$ in interactions of K^+ and π^+ mesons with Al and Au nuclei at 250 GeV/c, corresponding to the reactions

$$K^+ \text{ Al} \rightarrow K_S^0 + X, \quad (1)$$

$$K^+ \text{ Au} \rightarrow K_S^0 + X, \quad (2)$$

$$\pi^+ \text{ Al} \rightarrow K_S^0 + X, \quad (3)$$

$$\pi^+ \text{ Au} \rightarrow K_S^0 + X, \quad (4)$$

The results are obtained in an experiment using the CERN European Hybrid Spectrometer (EHS) and the Rapid Cycling Bubble Chamber (RCBC), which was filled with hydrogen and served as vertex and track detector. RCBC was equipped with two thin nuclear targets, one of aluminium and one of gold.

At present there are rather few published results on neutral strange particle production in hadron-nucleus collisions. The available experimental data either suffer from low statistics in bubble chamber experiments or from limited acceptance in counter experiments (see [1] for a review). In the NA35 experiment, neutral strange particle production was studied in $p\text{Au}$ and OAu interactions at 60 and 200 GeV per nucleon and $p\text{S}$ and SS interactions at 200 GeV per nucleon, in limited regions of Feynman- x_F and transverse momentum [2]. In the RISC spectrometer, $\pi^- A$ ($A = \text{C}, \text{Cu}, \text{Pb}$) interactions at 40

* Partially supported by grants from CPBP 01.06 and 01.09

¹ EEC Guest Scientist

² Onderzoeker IIKW, Brussels, Belgium, now at MPI, München

³ Bevoegdverklaard Navorser NFWO, Belgium

⁴ Now at Syracuse University, Syracuse NY 13244-1130, USA

GeV/c were examined in events triggered by high transverse momentum charged particles [3].

Unusually abundant production of strange particles has been advocated as a possible sign of quark-gluon plasma formation in nucleus-nucleus collisions. Therefore, besides its intrinsic interest, the production of neutral strange particles in the more elementary hadron-nucleus collisions at high energies can serve as a reference.

The paper is organized as follows. In Sect. 1 we describe the data sample and the procedures used to determine the cross sections for reactions (1–12). In Sect. 2 we present total inclusive cross sections and their A -dependence, and compare with two versions of the FRITIOF model. In Sect. 3 we discuss inclusive longitudinal and transverse momentum distributions. Our main conclusions are summarized in Sect. 4.

2 Experimental procedure

The experimental set-up of EHS and the trigger conditions are described in detail in [4]. The characteristics of the nuclear targets are described in [5]. Here, we mention only the details specific for the reactions studied. The neutral strange particles are detected as V^0 's in a cylindrical bubble chamber which has a diameter of 80 cm and depth 40 cm, wherein the nuclear targets are placed at 15.5 cm from the entrance window of the beam.

A total of about 2900 K^+ and 7500 π^+ events, candidate interactions in the foils, is measured. The sample of events, selected for this analysis, satisfies the following criteria

- the beam track is well measured and matches with the hits in the upstream wire chambers;
- the reconstructed vertex position is within one of the foils;
- the event is not a candidate for a quasi-elastic or coherent interaction;
- A quasi-elastic event is defined by the following criteria:
 1. the charge multiplicity equals two,
 2. the missing transverse momentum is less than 0.2 GeV/c,
 3. the missing longitudinal momentum is less than 9 GeV/c.
- A coherent interaction is defined by the requirements that

1. the charge multiplicity is odd and ≤ 5 ,
2. all charged particles have rapidities larger than one, if measured in the K^+ -nucleon c.m. system.

The number of accepted events amounts to 1211, 991, 3410 and 2834 for K^+ Al, K^+ Au, π^+ Al and π^+ Au interactions, respectively. The admixture of interactions in the hydrogen of the bubble chamber is estimated to be less than 4% in the Al and less than 2% in the Au sample. Microbarn equivalents are obtained by normalization of the number of events to the corresponding inelastic cross sections at 250 GeV/c [6].

Table 1. Pattern of 3C fit hypotheses for unique and ambiguous K_S^0 , Λ and $\bar{\Lambda}$ hypotheses in K^+ Al/Au and π^+ Al/Au interactions at 250 GeV/c, for the events in the fiducial volume. In brackets the number of V^0 's after the cut on minimum decay length

	K^+ Al	K^+ Au	π^+ Al	π^+ Au
γ	218	233	784	655
K_S^0	137(103)	121(83)	288(232)	346(272)
Λ	64(45)	77(53)	149(107)	200(142)
$\bar{\Lambda}$	11(8)	5(4)	13(11)	20(15)
K/γ	5	7	21	14
Λ/γ	13	6	26	18
$\bar{\Lambda}/\gamma$	10	10	25	27
$\Lambda/K/\gamma$	1	1	–	7
$\bar{\Lambda}/K/\gamma$	–	–	7	6
Λ/K	17	19	45	72
$\bar{\Lambda}/K$	5	6	11	11

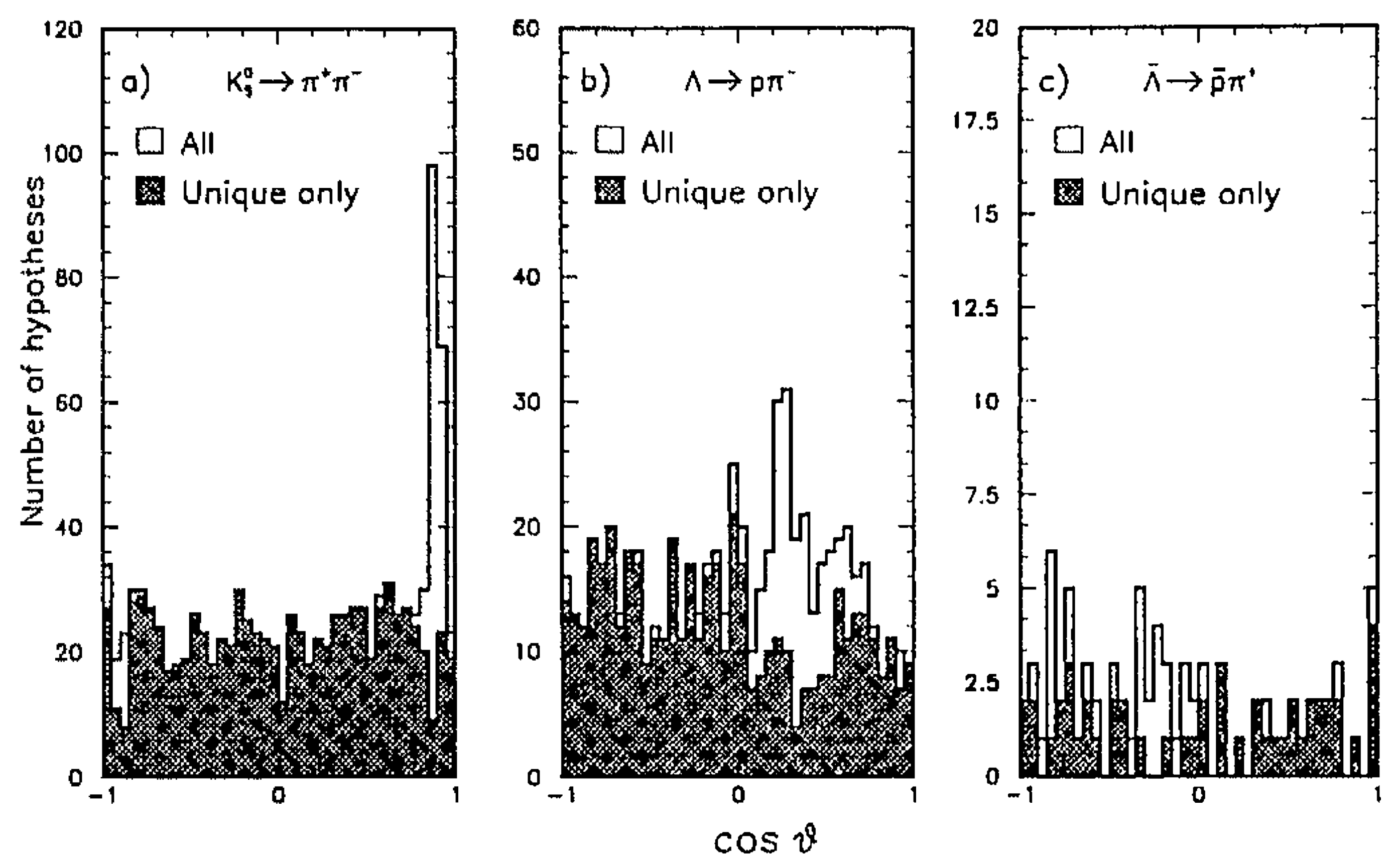


Fig. 1a–c. The distributions in $\cos\vartheta$ (see text) for unambiguous and ambiguous (shaded areas) V^0 's: a K_S^0 , b Λ and c $\bar{\Lambda}$, in the combined K^+ and π^+ samples

The selection of the sample of V^0 's and the calculation of their weights are made as described in previous papers [7, 8]. A restricted fiducial volume is defined in such a way that both tracks of the V^0 have a minimum length of 12 cm in the bubble chamber. Both tracks also must have opposite charge and a momentum uncertainty $\Delta p/p$ of less than 25%. The following four kinematical fit hypotheses are tried for each V^0 : $\gamma \rightarrow e^+ e^-$, $K_S^0 \rightarrow \pi^+ \pi^-$, $\Lambda^0 \rightarrow p \pi^-$ and $\bar{\Lambda}^0 \rightarrow \bar{p} \pi^+$. The number of K_S^0 , Λ and $\bar{\Lambda}$ in the fiducial volume, with unique and ambiguous 3C-fits, is listed in Table 1. V^0 's which are ambiguous with the γ hypothesis are considered to be γ 's. In Fig. 1 we show the distribution of the cosine of the decay angle ϑ for K_S^0 , Λ and $\bar{\Lambda}$ with ϑ the angle between the V^0 direction in the laboratory frame and the direction of the positive decay particle in the V^0 rest frame. In this paper, we only use unambiguous V^0 's. To correct for the loss due to the elimination of ambiguous ones, each V^0 is weighted with a momentum-dependent factor.

The K_S^0 , Λ and $\bar{\Lambda}$ mass distributions, calculated from the measured momenta of the decay tracks, for the combined K^+ and π^+ samples on both Al and Au, are shown

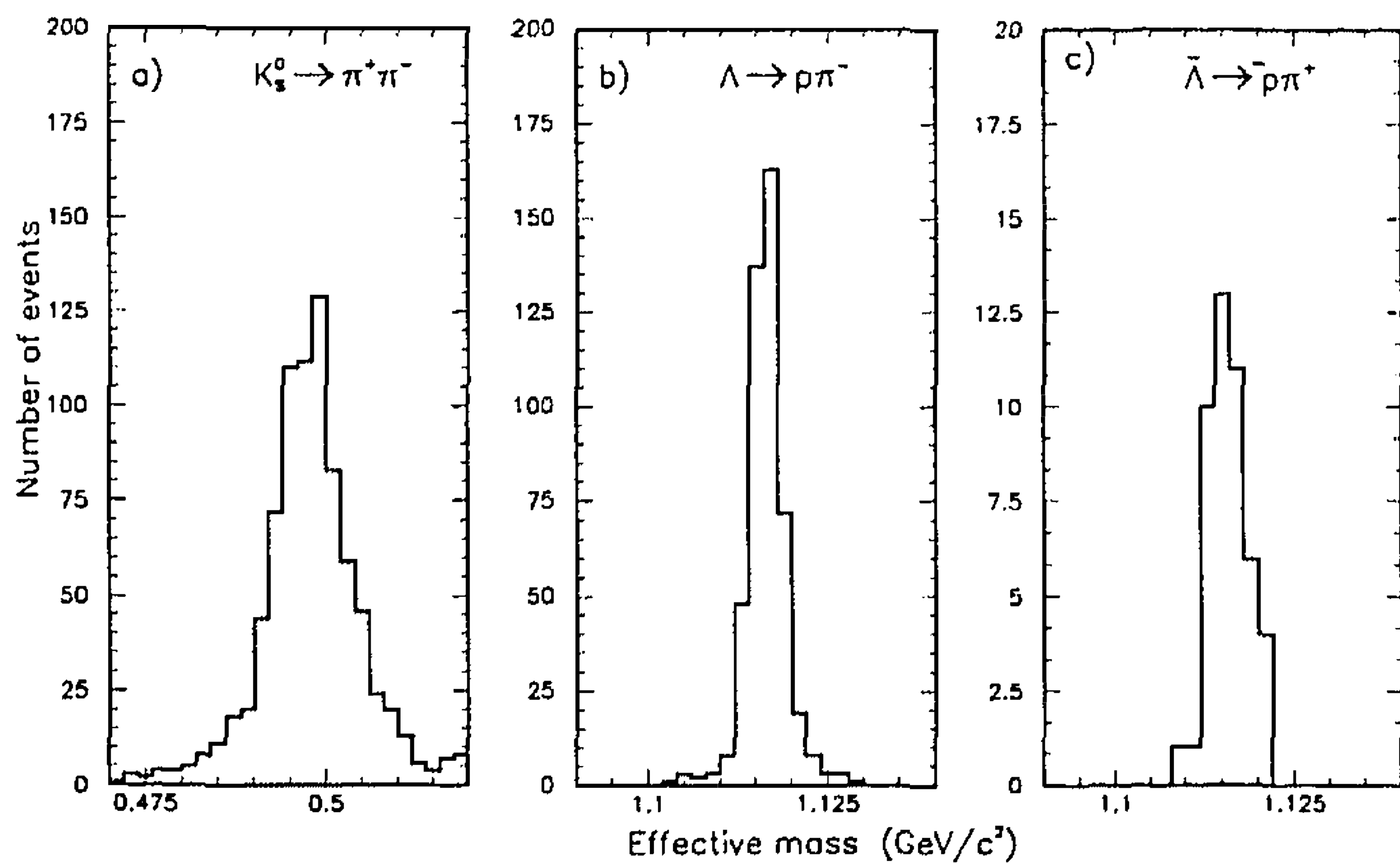


Fig. 2a-c. The K_S^0 , Λ and $\bar{\Lambda}$ effective mass distributions in the combined K^+ and π^+ samples

Table 2. The average K_S^0 , Λ and $\bar{\Lambda}$ weights in the reactions (1-12)

	K^+ Al	K^+ Au	π^+ Al	π^+ Au
$\langle W_{K_S^0} \rangle$	5.40	4.77	4.36	4.18
$\langle W_{\Lambda} \rangle$	4.79	4.73	5.48	4.80
$\langle W_{\bar{\Lambda}} \rangle$	10.33	8.24	8.00	6.42

in Fig. 2. The average effective mass value for K_S^0 , Λ and $\bar{\Lambda}$ is 497.8 ± 0.3 , 1115.9 ± 0.2 , 1115.7 ± 0.5 (MeV/c²), respectively, in good agreement with the values quoted by the Particle Data Group (PDG) [9]. The measured FWHM is found to be 7.1, 2.8 and 2.7 (MeV/c²).

All V^0 's are further assigned a weight factor to correct for the loss of decays outside the fiducial volume and for unseen decay modes. Furthermore, a momentum dependent minimum decay length is imposed. The numbers of K_S^0 , Λ and $\bar{\Lambda}$ selected for analysis, are shown in Table 1 in brackets. Cross sections are determined by multiplication of the summed V^0 weights with the corresponding microbarn equivalent. The average K_S^0 , Λ and $\bar{\Lambda}$ weights, which include all corrections, are shown in Table 2 for the reactions (1-12). Since the weight derived from the potential decay length becomes very large for energetic neutral strange particle decays, we restrict the data sample to the kinematical region $-1.0 < x_F < 0.1$ in the following analysis*. The available number of $\bar{\Lambda}$ -decays is too small to allow meaningful analyses and will therefore not be used.

3 Inclusive cross sections and their A dependence

The inclusive cross sections for reactions (1-8) in the interval $-1 < x_F < 0.1$ are collected in Table 3. The first error is statistical, the second systematical. In the remainder of the paper, all errors quoted are statistical.

* The Feynman variable x_F and rapidity y are calculated in the rest frame of the meson-nucleon system

The ratios $\sigma^{\pi^+ A} / \sigma^{K^+ A}$ for K_S^0 and Λ production, given in Table 3, are compatible within errors with the ratios of the inelastic π^+ and K^+ cross sections on Al and Au nuclei at 250 GeV/c [6]

$$\sigma_{\text{inel}}^{\pi^+ \text{Al}} / \sigma_{\text{inel}}^{K^+ \text{Al}} = 1.14 \pm 0.05, \quad (13)$$

$$\sigma_{\text{inel}}^{\pi^+ \text{Au}} / \sigma_{\text{inel}}^{K^+ \text{Au}} = 1.05 \pm 0.05.$$

In Table 4 we compare the average multiplicities of K_S^0 and Λ in K^+ and π^+ interactions on nuclei to those in "elementary" K^+p and π^+p interactions [7, 8]. Both $\langle K_S^0 \rangle$ and $\langle \Lambda \rangle$ are the same within errors for K^+ and for π^+ induced interactions on both nuclei. From Table 4 we observe that the average numbers of produced Λ 's on both targets and for both projectiles, are compatible within one standard deviation with the relation

$$\langle n_{\Lambda}(MA) \rangle = \langle n_{\Lambda}(Mp) \rangle \cdot \langle v_{\Lambda} \rangle, \quad (14a)$$

where M is either K^+ or π^+ and $\langle v_{\Lambda} \rangle$ is the average number of projectile collisions in the nucleus A , equal to 1.67 for Al and 2.61 for Au. In other words, the probability to produce a Λ in a meson-nucleus collision is proportional to the number of projectile collisions. For K_S^0 production in π^+ interactions, the analogous relation

$$\langle n_{K_S^0}(MA) \rangle = \langle n_{K_S^0}(Mp) \rangle \cdot \langle v_{\Lambda} \rangle \quad (14b)$$

is not observed: the experimental average number of produced K_S^0 's is systematically lower than the one expected from the average number of projectile collisions. These observations are in agreement with the ideas put forward in [13] about Λ retention and reinteractions of kaons (see also Sect. 5).

The cross sections for the reactions (1-8) as a function of atomic weight A are shown in Fig. 3a, b. The K^+p and π^+p data are taken from [7, 8] but restricted to the same kinematic interval of $-1.0 < x_F < 0.1$. The cross sections are well fitted by the expression

$$\sigma = \sigma_0 A^{\alpha}. \quad (15)$$

The fitted values for σ_0 and α are listed in Table 5. The slope parameter α is of the order of 0.9. A similar dependence is observed in $\pi^- A$ ($A = \text{C, Cu, Pb}$) interactions at 40 GeV/c [3].

The inclusive cross sections for reactions (1-8) are compared with the predictions of the quark-parton model FRITIOF [10] (version 3) and with a modified version FRITIOF' [7] of this model (see Table 3 and Fig. 3). The differences between the two versions of this model are:

- the value of the strangeness suppression parameter λ_s in the Lund fragmentation scheme JETSET 6.3 was taken to be 0.2 in FRITIOF and 0.3 in FRITIOF' (default values were taken for all other parameters);
- in FRITIOF', the momentum sharing function of the J -quark was modified to the form

$$f(x_J) = x_J(1-x_J)^{10}. \quad (16)$$

Table 3. The K_S^0 and Λ inclusive cross sections in reactions (1–8) in the interval $-1.0 < x_F < 0.1$, together with their ratio in K^+ and π^+ collisions on nuclei Al and Au. Predictions are given of two versions of the FRITIOF model (see text) for the cross sections in the same kinematic interval

Reaction	Experiment σ_{incl} (mb)	Model (mb)		$\sigma^{\pi^+ A} / \sigma^{K^+ A}$ (from exp.)
		FRITIOF	FRITIOF'	
$K^+ \text{Al} \rightarrow K_S^0 + X$	$74.9 \pm 8.6 \pm 7.5$	77	90	1.01 ± 0.15
$\pi^+ \text{Al} \rightarrow K_S^0 + X$	$75.7 \pm 5.7 \pm 7.6$	70	95	
$K^+ \text{Au} \rightarrow K_S^0 + X$	$412 \pm 53 \pm 41$	529	596	
$\pi^+ \text{Au} \rightarrow K_S^0 + X$	$457 \pm 30 \pm 46$	447	576	
$K^+ \text{Al} \rightarrow \Lambda + X$	$46.3 \pm 7.5 \pm 4.6$	27	40	0.95 ± 0.19
$\pi^+ \text{Al} \rightarrow \Lambda + X$	$44.0 \pm 4.8 \pm 4.4$	34	48	
$K^+ \text{Au} \rightarrow \Lambda + X$	$348 \pm 50 \pm 35$	205	282	0.97 ± 0.17
$\pi^+ \text{Au} \rightarrow \Lambda + X$	$336 \pm 32 \pm 34$	227	320	

Table 4. The average K_S^0 and Λ multiplicity per inelastic collision in the interval $-1.0 < x_F < 0.1$ for reactions (1–8), compared to that in $K^+ p$ and $\pi^+ p$ collisions. In the fourth and sixth columns, the average K_S^0 and Λ multiplicities computed according to (14) are given

Reaction	$\langle \pi^- \rangle$	$\langle K_S^0 \rangle$	$\langle K_S^0 \rangle$ from (14)	$\langle \Lambda \rangle$	$\langle \Lambda \rangle$ from (14)
$K^+ p$	2.78 ± 0.02	0.181 ± 0.019	input	0.082 ± 0.010	input
$\pi^+ p$	2.75 ± 0.02	0.184 ± 0.011	input	0.086 ± 0.012	input
$K^+ \text{Al}$	4.26 ± 0.16	0.260 ± 0.057	0.302 ± 0.032	0.161 ± 0.042	0.137 ± 0.017
$\pi^+ \text{Al}$	4.72 ± 0.13	0.231 ± 0.045	0.307 ± 0.032	0.134 ± 0.028	0.144 ± 0.020
$K^+ \text{Au}$	6.17 ± 0.24	0.299 ± 0.069	0.472 ± 0.050	0.252 ± 0.062	0.214 ± 0.026
$\pi^+ \text{Au}$	5.93 ± 0.22	0.316 ± 0.054	0.480 ± 0.050	0.232 ± 0.046	0.224 ± 0.031

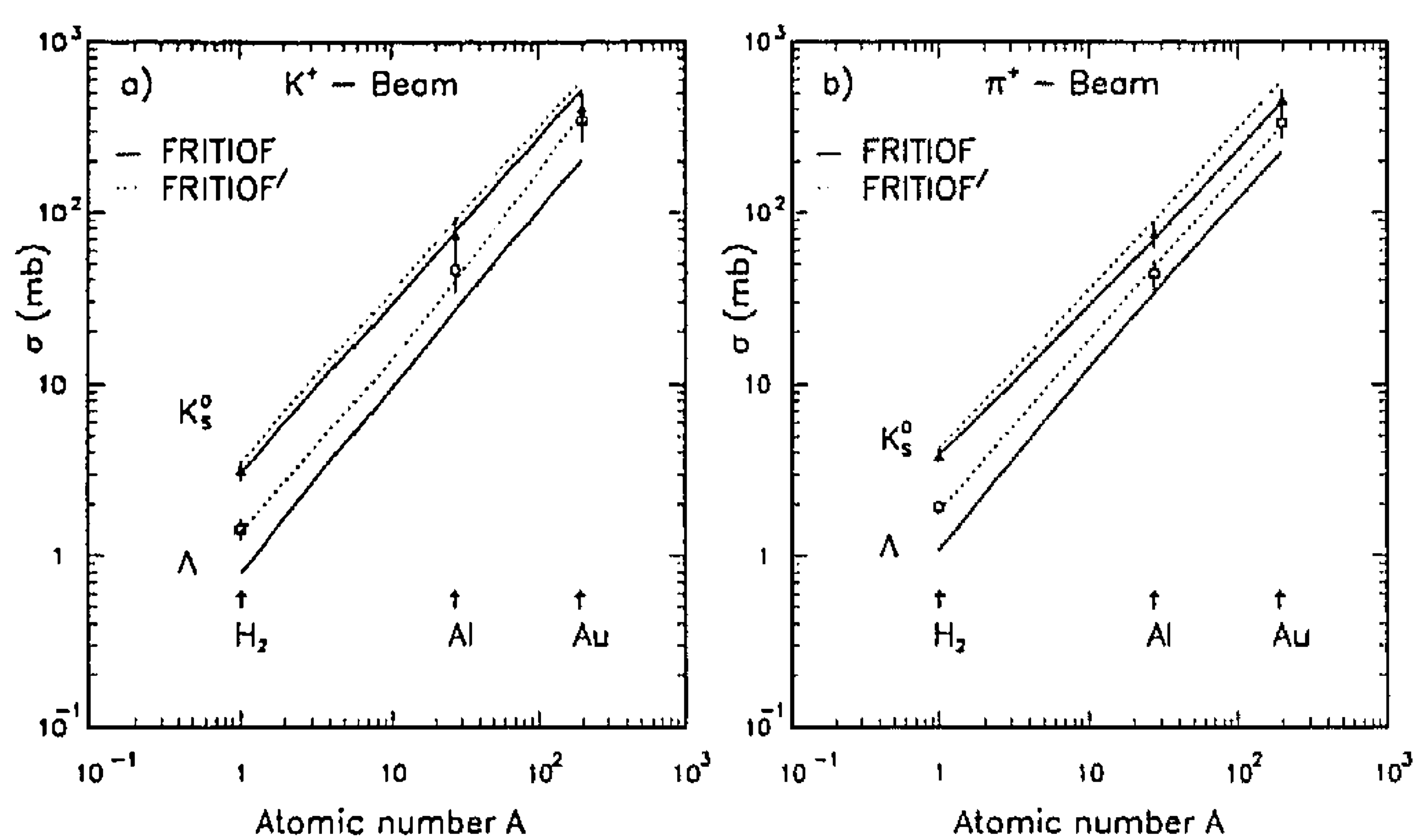


Fig. 3a, b. Cross sections for the reactions a (1–6) and b (7–12) as a function of the atomic number A , and predictions of the FRITIOF and FRITIOF' models. For Λ and $\bar{\Lambda}$ channels the cross sections are given in the interval $-1 < x_F < 0.1$, both for the data and the models

Table 5. Results of a fit with the expression $\sigma = \sigma_0 A^\alpha$ for the inclusive K_S^0 and Λ cross sections in K^+/π^+ interactions on $p/\text{Al}/\text{Au}$ at 250 GeV/c in $-1 < x_{F^0} < 0.1$

Beam	Particles	α	σ_0 (mb)
K^+	K_S^0	0.882 ± 0.043	3.981 ± 0.435
	Λ	1.041 ± 0.049	1.445 ± 0.197
π^+	K_S^0	0.979 ± 0.034	2.709 ± 0.266
	Λ	0.986 ± 0.044	1.786 ± 0.244

This was found necessary to describe the inclusive spectra of baryons in $\pi^+ p$ and $K^+ p$ interactions [7].

The predicted cross sections, based on 20,000 generated events per channel, are given in Table 3 and the dependence of the K_S^0 and Λ cross sections on atomic weight A is shown in Fig. 3a, b. Both versions of the model correctly predict the A -dependence of the Λ production cross section in reactions (5) to (8) but the cross section values are considerably better reproduced by the modified version of the model. The cross sections for K_S^0 in interactions on Al are reasonably well predicted by both versions of the model. However, a too high cross section is predicted by FRITIOF' for K_S^0 production in $K^+ \text{Au}$ interactions.

Table 6. Inclusive cross sections for events with two V^0 -particles in the final state in $K^+ \text{Al}/\text{Au}$ and $\pi^+ \text{Al}/\text{Au}$ interactions at 250 GeV/c; the number of events is given in brackets

Final particles	Cross sections (mb)			
	$K^+ \text{Al}$	$K^+ \text{Au}$	$\pi^+ \text{Al}$	$\pi^+ \text{Au}$
$K_S^0 K_S^0$	17 ± 7 (6)	202 ± 91 (7)	15 ± 4 (14)	107 ± 29 (17)
$\Lambda \Lambda$	30 ± 19 (3)	81 ± 63 (2)	1.7 ± 1.2 (2)	28 ± 16 (3)
$K_S^0 \Lambda$	28 ± 11 (8)	209 ± 89 (7)	17 ± 5 (17)	282 ± 77 (27)

Table 6 gives the inclusive cross sections of K^+ and π^+ interactions on Al and Au nuclei for channels with two neutral strange particles in full phase space (the number of events is given in brackets). For events with two K_S^0 mesons, the parametrization (15) yields values of the slope parameter $\alpha = 0.92 \pm 0.14$ and 0.90 ± 0.06 for K^+ and π^+ beams, respectively. They are equal within errors to those for inclusive K_S^0 production.

4 Inclusive spectra

4.1 Feynman- x and rapidity distributions

Feynman x_F and rapidity y are calculated in the c.m.s. of the projectile and a nucleon of the nucleus. The Feynman- x_F distributions for K_S^0 and Λ production are shown in Figs. 4 and 5, the rapidity distributions are given in Table 7.

Figure 4 shows that the K_S^0 spectra up to $x_F=0.1$ are very similar in K^+ and in π^+ induced reactions on Al, as well on the heavy Au nucleus. Both versions of the FRITIOF model describe K_S^0 production (Fig. 4) reasonably well. Exceptions are reactions on Au in the target fragmentation region, where the models predict a too low cross section, and K^+ Au interactions in the central region, where the model is too high.

The Λ -hyperons in the reactions (5) to (8) are primarily produced from target fragmentation. As for collisions on hydrogen [7], the FRITIOF model predicts a double bump structure of the $d\sigma/dx$ spectra of the Λ -hyperons which is not observed experimentally (see

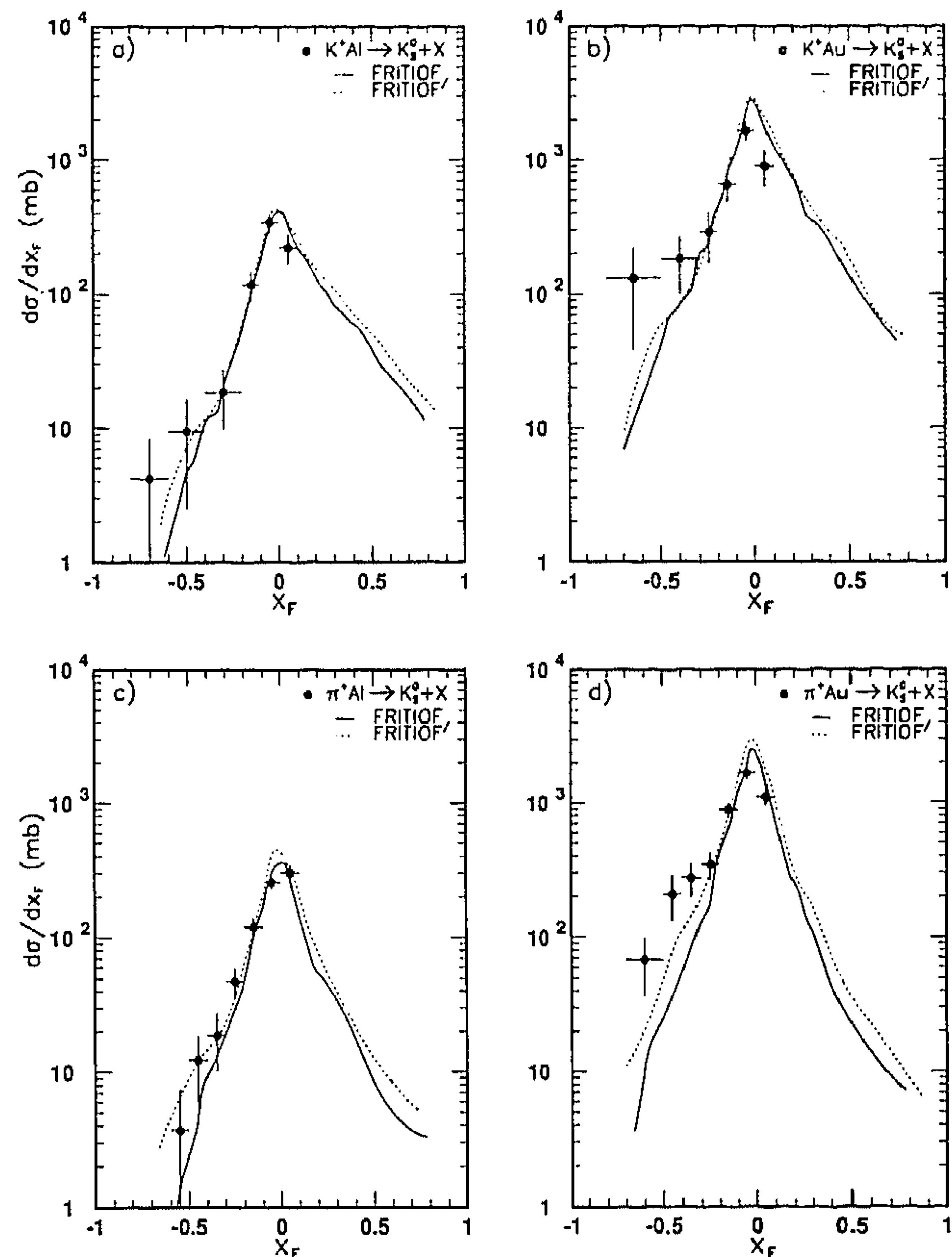


Fig. 4a-d. Feynman- x_F distributions for K_S^0 production in a K^+ Al, b K^+ Au, c π^+ Al and d π^+ Au interactions. The curves are predictions of the quark-parton models FRITIOF (full line) and FRITIOF' (dotted line)

Table 7. Differential cross section $d\sigma/dy$ (in mb) for K_S^0 and Λ production in K^+ Al, K^+ Au, π^+ Al and π^+ Au collisions

K^+ Al		K^+ Au		π^+ Al		π^+ Au	
interval	$d\sigma/dy$	interval	$d\sigma/dy$	interval	$d\sigma/dy$	interval	$d\sigma/dy$
K_S^0							
-2.8 ↔ -2.4	5.2 ± 3.7	-3.2 ↔ -2.4	70.1 ± 38.6	-2.8 ↔ -2.4	8.5 ± 2.9	-3.4 ↔ -2.6	31.1 ± 11.8
-2.4 ↔ -2.0	9.6 ± 4.5	-2.4 ↔ -2.0	71.0 ± 29.2	-2.4 ↔ -2.0	8.0 ± 2.3	-2.6 ↔ -2.2	96.0 ± 21.4
-2.0 ↔ -1.6	22.6 ± 6.3	-2.0 ↔ -1.6	96.0 ± 34.6	-2.0 ↔ -1.6	14.1 ± 3.2	-2.2 ↔ -1.8	119.2 ± 22.6
-1.6 ↔ -1.2	12.7 ± 4.5	-1.6 ↔ -1.2	146.8 ± 39.7	-1.6 ↔ -1.2	15.3 ± 3.3	-1.8 ↔ -1.4	116.5 ± 21.4
-1.2 ↔ -0.8	20.4 ± 6.3	-1.2 ↔ -0.8	149.0 ± 41.7	-1.2 ↔ -0.8	17.2 ± 3.5	-1.4 ↔ -1.0	120.7 ± 21.4
-0.8 ↔ -0.4	31.6 ± 7.7	-0.8 ↔ -0.4	129.6 ± 39.3	-0.8 ↔ -0.4	28.3 ± 4.5	-1.0 ↔ -0.6	131.2 ± 22.9
-0.4 ↔ 0.0	29.2 ± 8.7	-0.4 ↔ 0.0	103.3 ± 34.6	-0.4 ↔ 0.0	22.8 ± 4.3	-0.6 ↔ -0.2	164.2 ± 26.1
0.0 ↔ 0.4	18.7 ± 6.9	0.0 ↔ 0.4	72.2 ± 32.9	0.0 ↔ 0.4	27.6 ± 5.1	-0.2 ↔ 0.2	123.3 ± 26.5
0.4 ↔ 0.8	18.7 ± 7.3	0.4 ↔ 0.8	96.2 ± 43.3	0.4 ↔ 0.8	18.8 ± 5.2	0.2 ↔ 0.6	159.3 ± 31.4
0.8 ↔ 1.2	19.2 ± 10.0	0.8 ↔ 2.0	79.8 ± 34.7	0.8 ↔ 1.2	19.7 ± 7.2	0.6 ↔ 1.4	88.7 ± 22.8
1.2 ↔ 2.0	32.8 ± 10.8			1.2 ↔ 1.6	15.4 ± 6.2	1.4 ↔ 2.6	69.5 ± 27.5
2.0 ↔ 3.2	25.5 ± 14.2			1.6 ↔ 2.0	11.3 ± 5.7		
				2.0 ↔ 2.4	8.0 ± 5.7		
Λ							
-3.0 ↔ -2.6	7.3 ± 4.3	-3.0 ↔ -2.6	125.6 ± 42.9	-3.4 ↔ -3.0	1.8 ± 1.3	-3.2 ↔ -3.0	30.3 ± 16.4
-2.6 ↔ -2.2	15.6 ± 5.6	-2.6 ↔ -2.2	121.9 ± 41.9	-3.0 ↔ -2.6	8.5 ± 2.9	-3.0 ↔ -2.6	133.4 ± 25.4
-2.2 ↔ -1.8	30.2 ± 8.2	-2.2 ↔ -1.8	200.6 ± 59.4	-2.6 ↔ -2.2	11.7 ± 3.0	-2.6 ↔ -2.2	161.6 ± 28.8
-1.8 ↔ -1.0	15.8 ± 4.7	-1.8 ↔ -1.0	101.2 ± 28.9	-2.2 ↔ -1.8	20.2 ± 4.3	-2.2 ↔ -1.8	146.7 ± 30.4
-1.0 ↔ 0.2	10.9 ± 4.3	-1.0 ↔ 0.2	76.5 ± 25.6	-1.8 ↔ -1.4	23.0 ± 5.1	-1.8 ↔ -1.4	106.7 ± 25.0
				-1.4 ↔ -1.0	8.6 ± 2.9	-1.4 ↔ -1.0	85.6 ± 23.2
				-1.0 ↔ -0.2	10.6 ± 2.8	-1.0 ↔ -0.2	34.2 ± 11.7
				-0.2 ↔ 1.0	8.5 ± 3.2	-0.6 ↔ 0.2	52.8 ± 20.5
						0.6 ↔ 1.4	22.6 ± 18.3

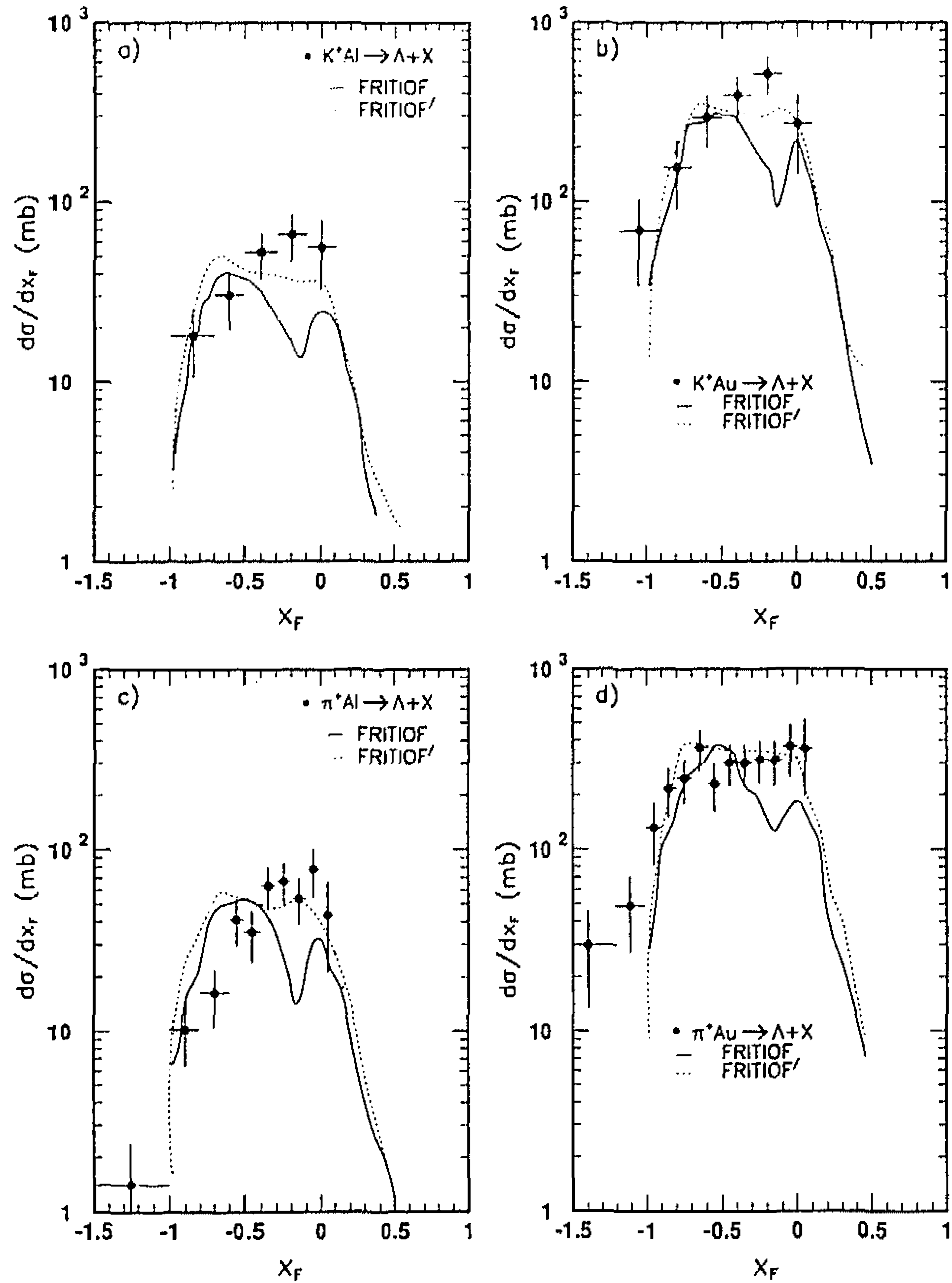


Fig. 5a-d. As in Fig. 4, for Λ production

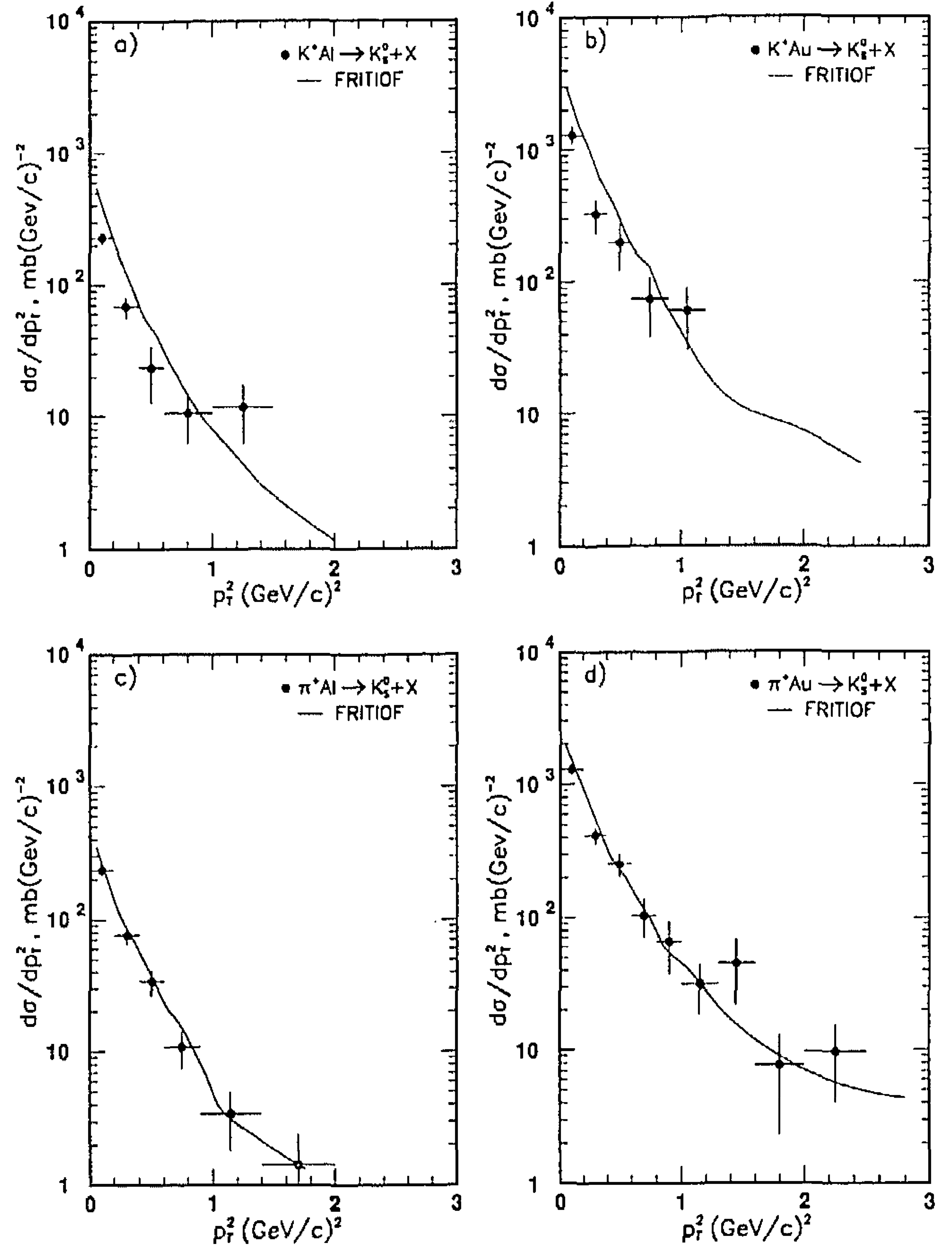


Fig. 6a-d. p_T^2 distributions for K_S^0 production in a K^+Al , b K^+Au , c π^+Al and d π^+Au interactions. The curves are predictions from the FRITIOF model

Fig. 5). The changes introduced into the FRITIOF' model, in particular the modified momentum-sharing function of the J -quark (15), eliminate this double-bump dependence, resulting in a better agreement with the experimental data.

The authors of [2] have found a considerably larger Λ -hyperon yield in heavy ion interactions in the central region as compared to the standard version of the FRITIOF model. This enhancement, relative to the model, is also observed in our data (see Fig. 5) but it is no more present in FRITIOF', confirming the conclusion in [7] that a much softer J -quark distribution is needed in the Lund jet fragmentation scheme JETSET 6.3 in order to describe baryon production.

4.2 Transverse momentum distributions

Figures 6 and 7 present the distributions in the transverse momentum squared, $d\sigma/dp_T^2$, for K_S^0 and Λ in the reactions (1-8). The values of $\langle p_T \rangle$ and $\langle p_T^2 \rangle$ are given in Table 8. The results of a fit to a single exponential form $a \exp(-bp_T^2)$ are given in Table 9. As seen from Table 9, the values of the slope parameters are the same within errors for interactions on Al as on Au nuclei and for π^+ interactions as for K^+ interactions. This holds separately for K_S^0 and for Λ production. The p_T^2 -distributions as a function of the transverse mass $m_T = (m_{p_0}^2 + p_T^2)^{1/2}$ are very well described by the form $a \exp(-bm_T)$ with the

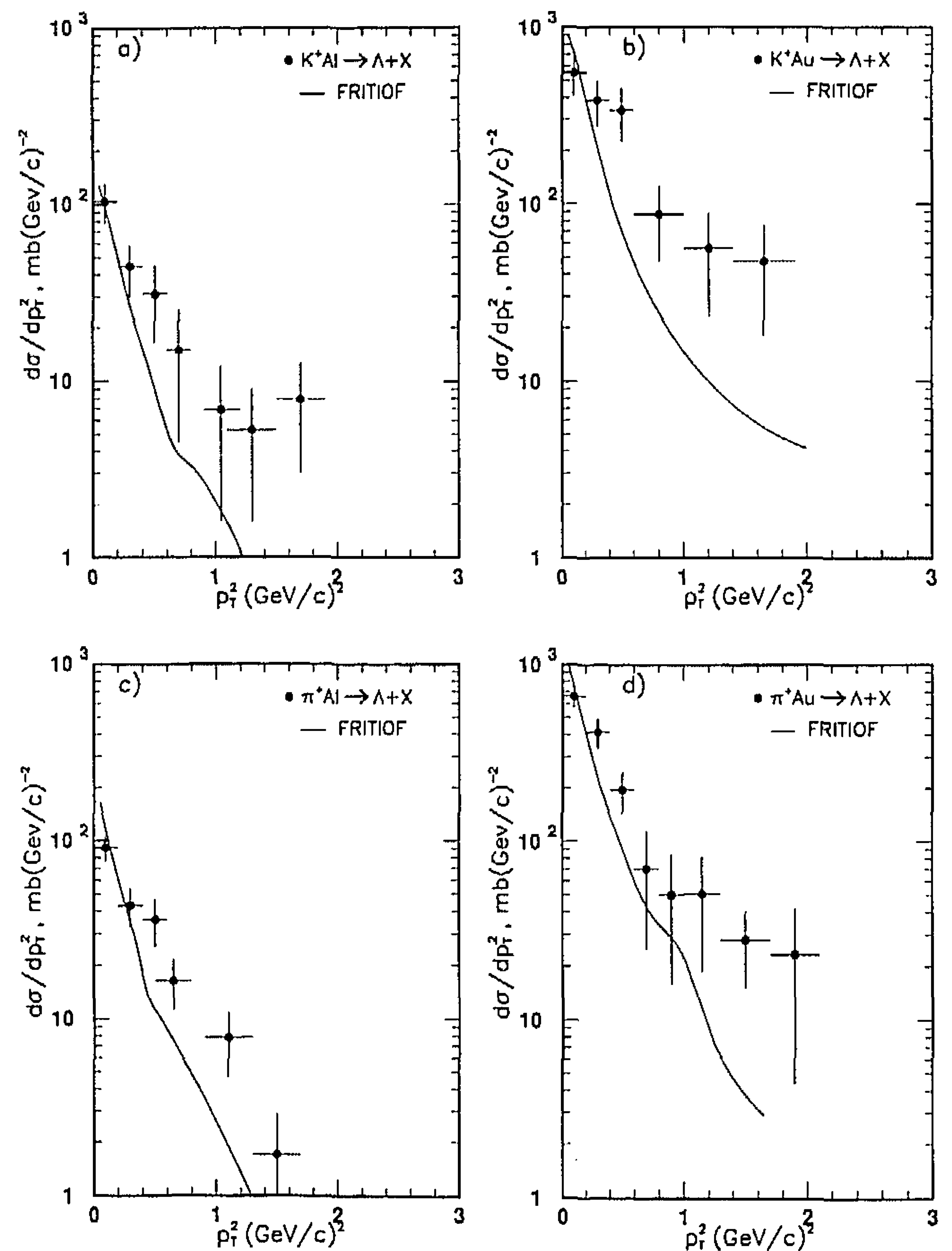


Fig. 7a-d. As in Fig. 6, for Λ production

parameters given in Table 10. The slope parameters in this parametrization are the same, within the measurement accuracy, for interactions on Al and Au.

Both versions of the FRITIOF model* describe fairly well the p_T^2 -distributions of K_S^0 's but fail to reproduce the Λ -spectrum at large p_T^2 .

The transverse spin polarization P_Λ of the Λ^0 in the K^+ -induced reactions (5) plus (6) and in the π^+ induced reactions (7) plus (8) was determined, using the same method as in [7] for interactions on protons. In K^+ collisions the polarization is found to be $P_\Lambda = -0.78 \pm 0.39$ (-0.54 ± 0.45) for $p_T(\Lambda)$ smaller (larger) than 0.5 GeV/c. In π^+ collisions, the numbers are $P_\Lambda = 0.18 \pm 0.24$ and $P_\Lambda = -0.41 \pm 0.28$, respectively.

5 Ratios of strange particle to π^- production

A dramatic increase in the ratio of strange to non-strange particles produced, is considered to be a possible signal of the formation of a quark-gluon plasma (QGP) in high energy heavy ion collisions. Data from a variety of interactions where no QGP is formed, are needed as a reference basis, in order to assess whether a significant increase is observed. Table 11 gives the ratio $R = \langle K_S^0 \rangle / \langle \pi^- \rangle$ for K^+ and π^+ interactions on protons, Al and Au, integrated over the interval $-1.0 < x_F < 0.1$. All negative particles are taken to be pions, except identified electrons with momentum less than 200 MeV/c.

* Because the p_T -structure of both versions of the model is identical, we show in Figs. 8 and 9 only predictions of the model with default parameter values, except $\lambda_s = 0.2$

Table 8. The average values of $\langle p_T \rangle$ and $\langle p_T^2 \rangle$ for K_S^0 and Λ in reactions (1-8) in the kinematical interval $-1.0 < x_F < 0.1$

Interaction	Particles	$\langle p_T \rangle$ (GeV/c)	$\langle p_T^2 \rangle$ (GeV/c) ²
K^+ Al	K_S^0	0.466 ± 0.034	0.304 ± 0.047
	Λ	0.569 ± 0.055	0.438 ± 0.080
K^+ Au	K_S^0	0.446 ± 0.040	0.298 ± 0.062
	Λ	0.649 ± 0.051	0.543 ± 0.087
π^+ Al	K_S^0	0.423 ± 0.022	0.268 ± 0.035
	Λ	0.563 ± 0.036	0.424 ± 0.053
π^+ Au	K_S^0	0.467 ± 0.019	0.312 ± 0.027
	Λ	0.592 ± 0.034	0.482 ± 0.058

Table 9. Fits of the $d\sigma/dp_T^2$ distributions for K_S^0 and Λ in K^+ Al/Au and π^+ Al/Au interactions at 250 GeV/c to the form $a \exp(-bp_T^2)$

Interaction	Particles	p_T^2 interval (GeV/c) ²	a mb(GeV/c) ⁻²	b (GeV/c) ⁻²	χ^2/NDF
K^+ Al	K_S^0	0.0-1.5	351 ± 96	5.2 ± 0.7	5.5/3
	Λ	0.0-1.9	117 ± 31	2.7 ± 0.6	2.9/5
K^+ Au	K_S^0	0.0-1.2	1647 ± 368	4.5 ± 0.7	4.7/3
	Λ	0.0-1.9	695 ± 165	2.0 ± 0.4	2.6/4
π^+ Al	K_S^0	0.0-1.4	346 ± 41	4.7 ± 0.4	1.9/3
	Λ	0.0-1.7	112 ± 17	2.7 ± 0.3	1.4/4
π^+ Au	K_S^0	0.0-2.0	1660 ± 177	3.9 ± 0.3	10.4/6
	Λ	0.0-2.1	854 ± 121	2.8 ± 0.4	4.6/6

Table 10. Exponents b from fits of the $d\sigma/dm_T$ distributions for K_S^0 and Λ in K^+ Al/Au and π^+ Al/Au interactions at 250 GeV/c to the form $a \exp(-bm_T)$

Interaction	Particles	Interval m_T GeV	b GeV ⁻¹	χ^2/NDF
K^+ Al	K_S^0	0.497-1.3	6.9 ± 0.9	1.1/3
	Λ	1.115-1.8	6.6 ± 1.3	4.1/3
K^+ Au	K_S^0	0.497-1.2	6.7 ± 1.0	2.1/3
	Λ	1.115-2.1	5.2 ± 0.8	1.8/3
π^+ Al	K_S^0	0.497-1.5	7.1 ± 1.4	1.8/4
	Λ	1.115-1.7	6.6 ± 0.8	2.3/2
π^+ Au	K_S^0	0.497-1.5	5.9 ± 0.4	4.2/5
	Λ	1.115-2.0	6.3 ± 0.6	2.6/4

Table 11. Relative production rate of K_S^0 to π^- in K^+A and π^+A collisions in the kinematical interval $-1 < x_F < 0.1$

Interaction	$\langle K_S^0 \rangle / \langle \pi^- \rangle$
$K^+ p$	0.065 ± 0.007
$K^+ \text{Al}$	0.061 ± 0.014
$K^+ \text{Au}$	0.049 ± 0.011
$\pi^+ p$	0.067 ± 0.004
$\pi^+ \text{Al}$	0.055 ± 0.010
$\pi^+ \text{Au}$	0.053 ± 0.009

The relative production rate is about 5% in all channels; thus no increase in the relative production rate of K^0 's is observed off nuclei w.r.t. elementary collisions.

The Feynman- x_F dependence of the ratio

$$R(x_F) = \frac{d\sigma(K_S^0)}{dx_F} \bigg/ \frac{d\sigma(\pi^-)}{dx_F} \quad (17)$$

is presented in Fig. 8. The results for K^+p and π^+p reactions [8] are shown by full lines. In all cases the rate is smaller in meson-nucleus than in elementary interactions. The rates are the same in K^+ interactions on both nuclei in the central and target fragmentation regions. The latter observation also holds for π^+ collisions.

The relative production rate

$$R(p_T^2) = \frac{d\sigma(K_S^0)}{dp_T^2} \bigg/ \frac{d\sigma(\pi^-)}{dp_T^2} \quad (18)$$

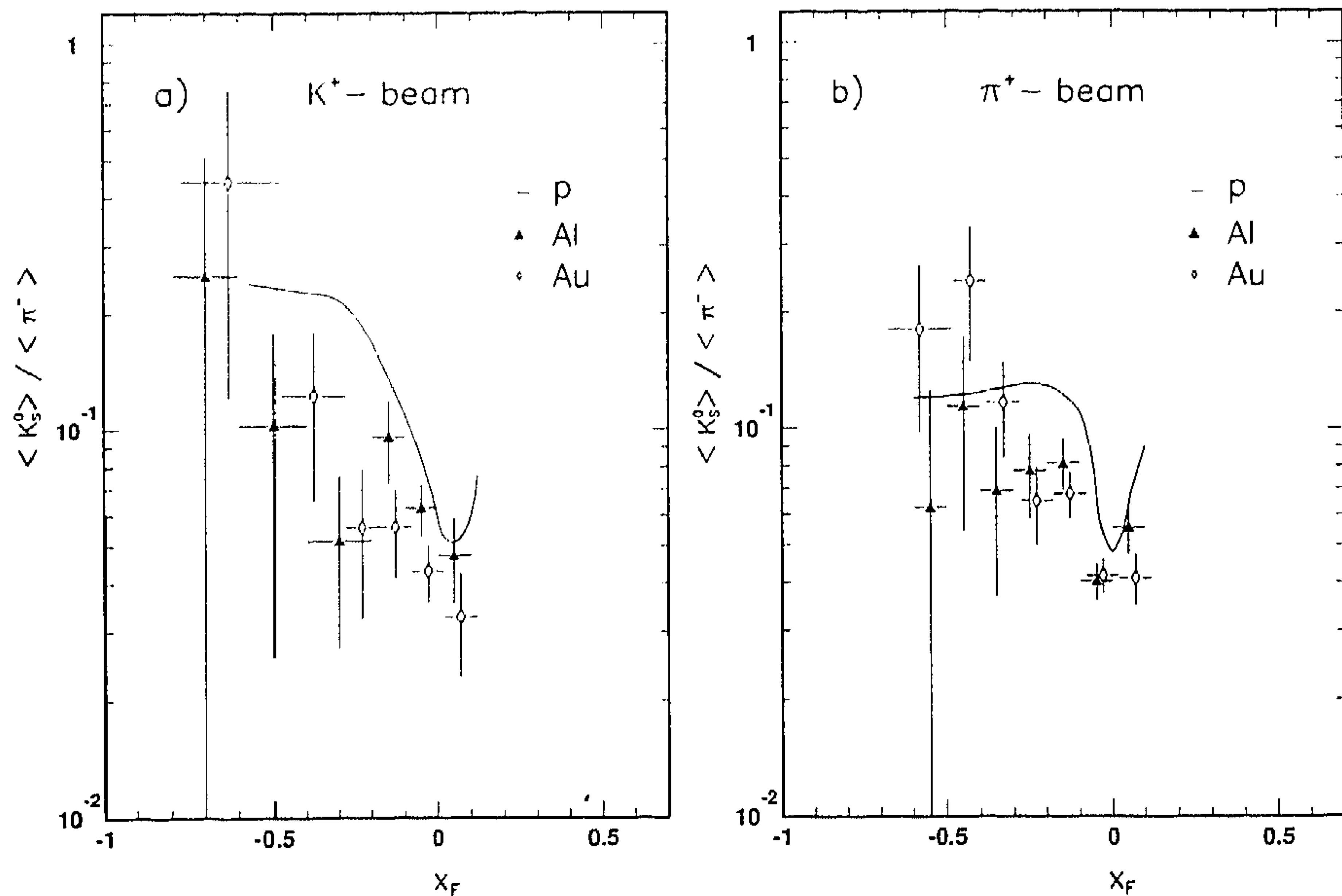


Fig. 8a, b. The ratio $R(x_F)$ of K_S^0 to π^- production as a function of x_F .

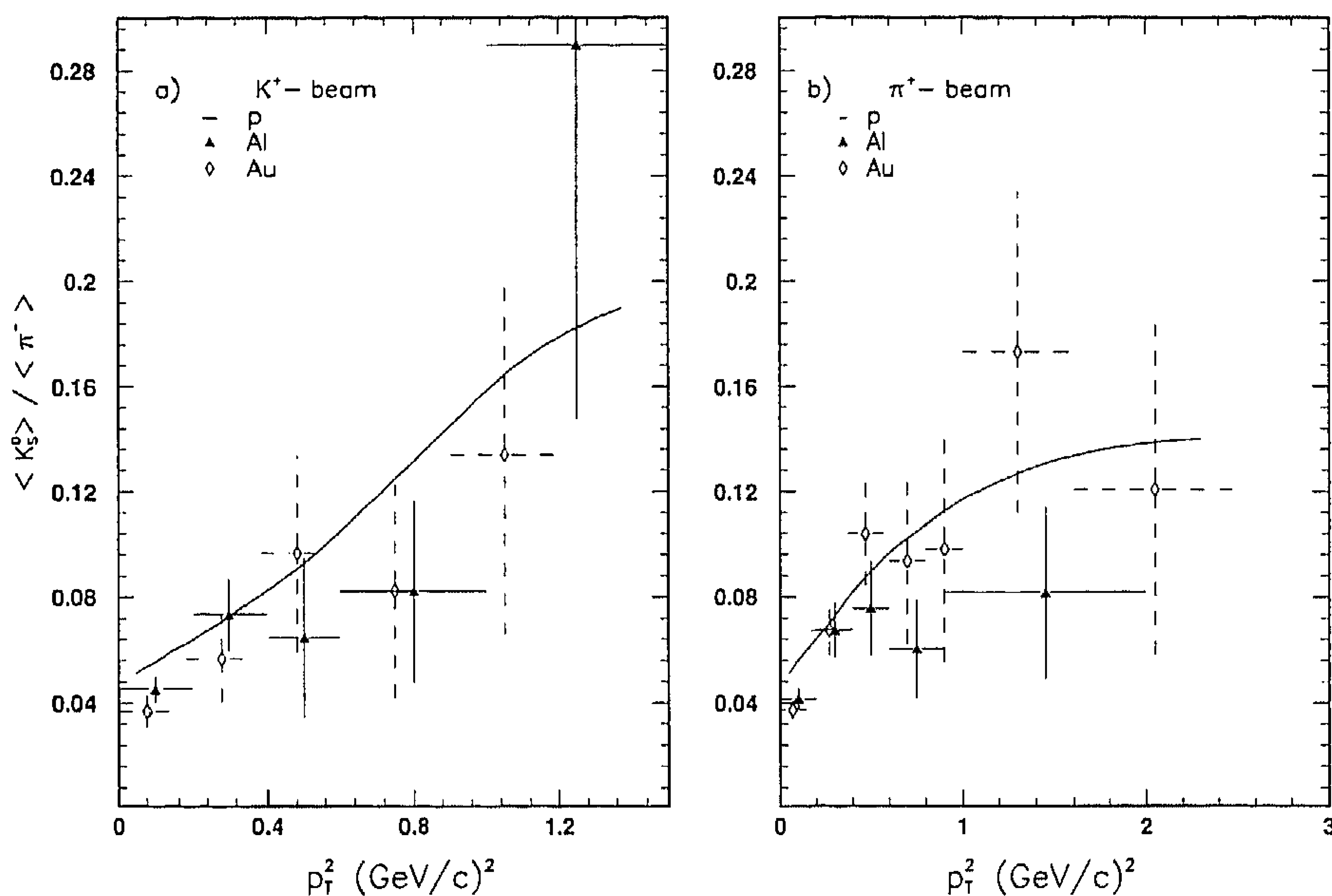


Fig. 9a, b. The ratio $R(p_T^2)$ of K_S^0 to π^- production as a function of p_T^2 .

is shown in Fig. 9. Full lines in Fig. 9a and b are the data for K^+p and π^+p interactions, respectively. The p_T^2 -dependence in meson-nucleus collisions follows the same trend as in elementary collisions; the K^0/π^- ratio increases with increasing p_T^2 .

In Sect. 3 we observed that the average number of produced Λ 's is proportional to the average number of projectile collisions and thus follows (14a), whereas this does not hold for produced K_S^0 's. The same observation was made in [12], based on pAr , pXe and $\bar{p}Xe$ interactions at 200 GeV/c. Preliminary results of the latter experiment led Nikolaev [13] to the concept of " Λ retention property" of nuclear interactions, which can be stated simply as follows: a Λ produced via fragmentation of a nucleon in the nucleus is not absorbed, but the

K^0/\bar{K}^0 can reinteract and thereby disappear or even produce a Λ . Based on these considerations, Nikolaev predicts a number of properties of events containing a Λ^0 as compared to minimum bias (MB) events, i.e. they are expected to have

- a high central plateau, thus larger charge multiplicity $\langle n_c \rangle$;
- larger average number of protons $\langle n_p \rangle$ and of grey protons $\langle n_g \rangle$ i.e. protons with $0.2 < \beta < 0.7$;
- a relatively narrower multiplicity distribution: $D_c/\langle n_c \rangle$ smaller;
- increasing $\langle n_\Lambda \rangle$ with increasing n_p or n^- .

We have checked these expectations by calculating the quantities $\langle n_p \rangle$, $\langle n_c \rangle$ and $D_c/\langle n_c \rangle$ in the four available

Table 12. Comparison of events with a K_S^0 or a Λ and minimum bias events

Reaction	Events	$\langle n_p \rangle$	$\langle n_c \rangle$	D_c	$D_c / \langle n_c \rangle$
$K^+ \text{Al}$	all	1.11 ± 0.03	12.84 ± 0.21	7.13 ± 0.66	0.56 ± 0.05
	K_S^0	1.60 ± 0.23	15.34 ± 0.79	7.03 ± 2.53	0.46 ± 0.17
	Λ	1.25 ± 0.22	15.83 ± 1.43	9.44 ± 4.52	0.60 ± 0.29
$K^+ \text{Au}$	all	3.17 ± 0.16	19.49 ± 0.46	13.30 ± 1.18	0.68 ± 0.06
	K_S^0	4.89 ± 0.70	28.44 ± 1.70	14.04 ± 5.20	0.49 ± 0.19
	Λ	4.72 ± 0.70	25.34 ± 1.65	10.87 ± 5.80	0.43 ± 0.23
$\pi^+ \text{Al}$	all	1.16 ± 0.02	12.90 ± 0.13	7.02 ± 0.39	0.54 ± 0.03
	K_S^0	1.44 ± 0.08	15.74 ± 0.56	7.97 ± 1.80	0.51 ± 0.12
	Λ	1.43 ± 0.14	16.78 ± 0.88	8.85 ± 2.75	0.53 ± 0.17
$\pi^+ \text{Au}$	all	3.04 ± 0.05	19.74 ± 0.27	13.20 ± 0.70	0.67 ± 0.04
	K_S^0	4.04 ± 0.16	25.60 ± 0.90	13.62 ± 2.66	0.53 ± 0.11
	Λ	5.32 ± 0.26	31.33 ± 1.28	14.29 ± 4.25	0.46 ± 0.14

channels for minimum bias events ("all"), for events with a K_S^0 and for events with a Λ^0 . The results, given in Table 12, lead to the following conclusions:

1. $\langle n_p \rangle$ is indeed larger in Λ events than in MB events, but it is also larger in K_S^0 events.
2. $\langle n_c \rangle$ is indeed larger in Λ events than in MB events, but also in K_S^0 events.
3. $D_c / \langle n_c \rangle$ is indeed smaller (for the heavy Au nucleus) in Λ events than in MB events, but so it is also in K_S^0 events.

From this we may conclude that strangeness production in general (and not particularly Λ production) is accompanied by more protons and more charged particles; in other words strangeness is on average produced in more central collisions.*

The last question which we address here is whether relatively more strangeness is produced in central collisions.

* This can naively be expected if one considers that production of "rarer" particles requires more energy to be dumped in the interaction volume

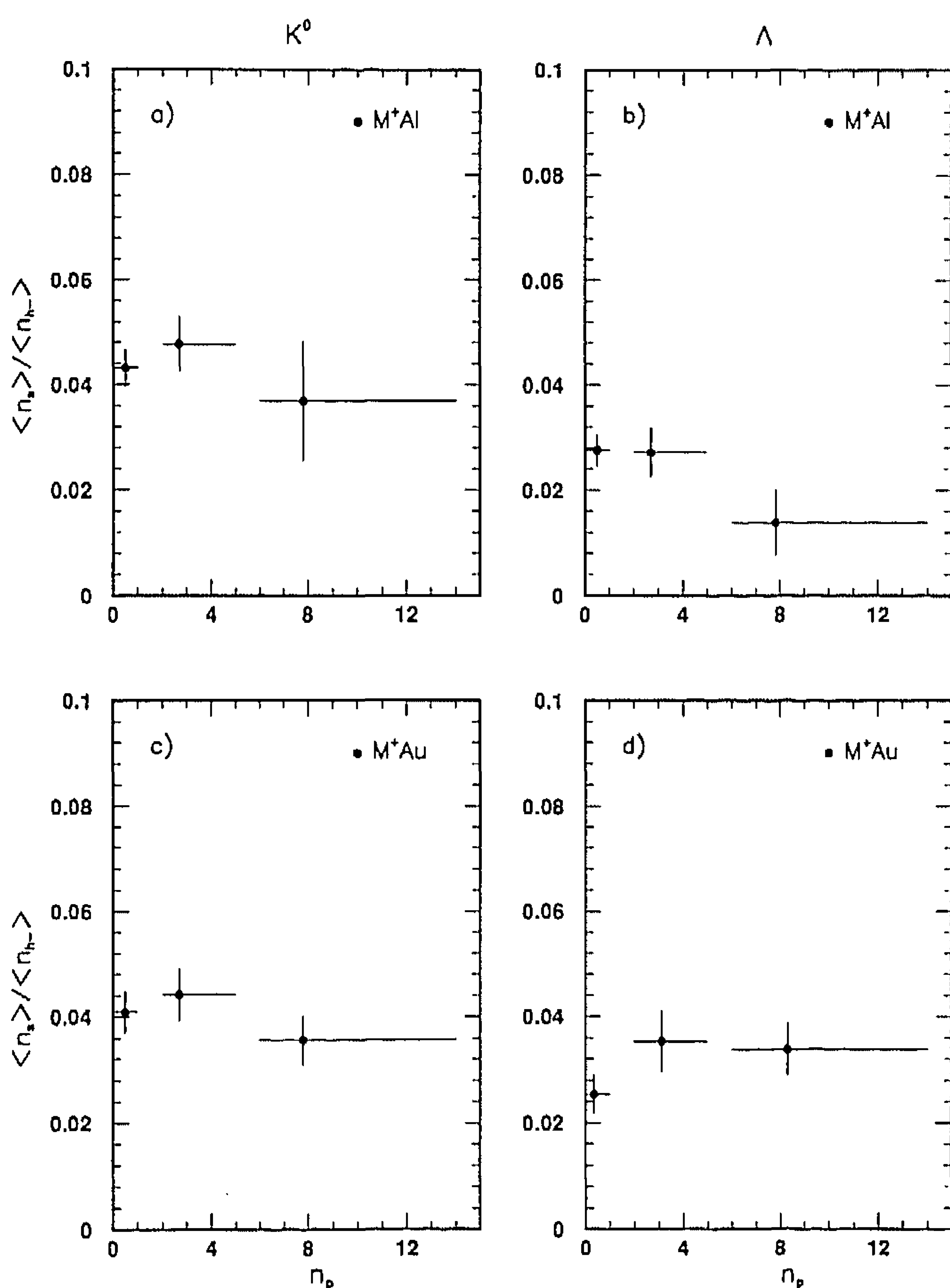


Fig. 10a-d. The relative production rate $\langle n_s \rangle / \langle n_{h^-} \rangle$ as a function of n_p , the number of protons, with $s = K^0$ ($s = \Lambda$) in **a, b** $M^+ \text{Al}$ and **c, d** in $M^+ \text{Au}$ collisions. M^+ stands for the combined sample of K^+ and π^+ interactions

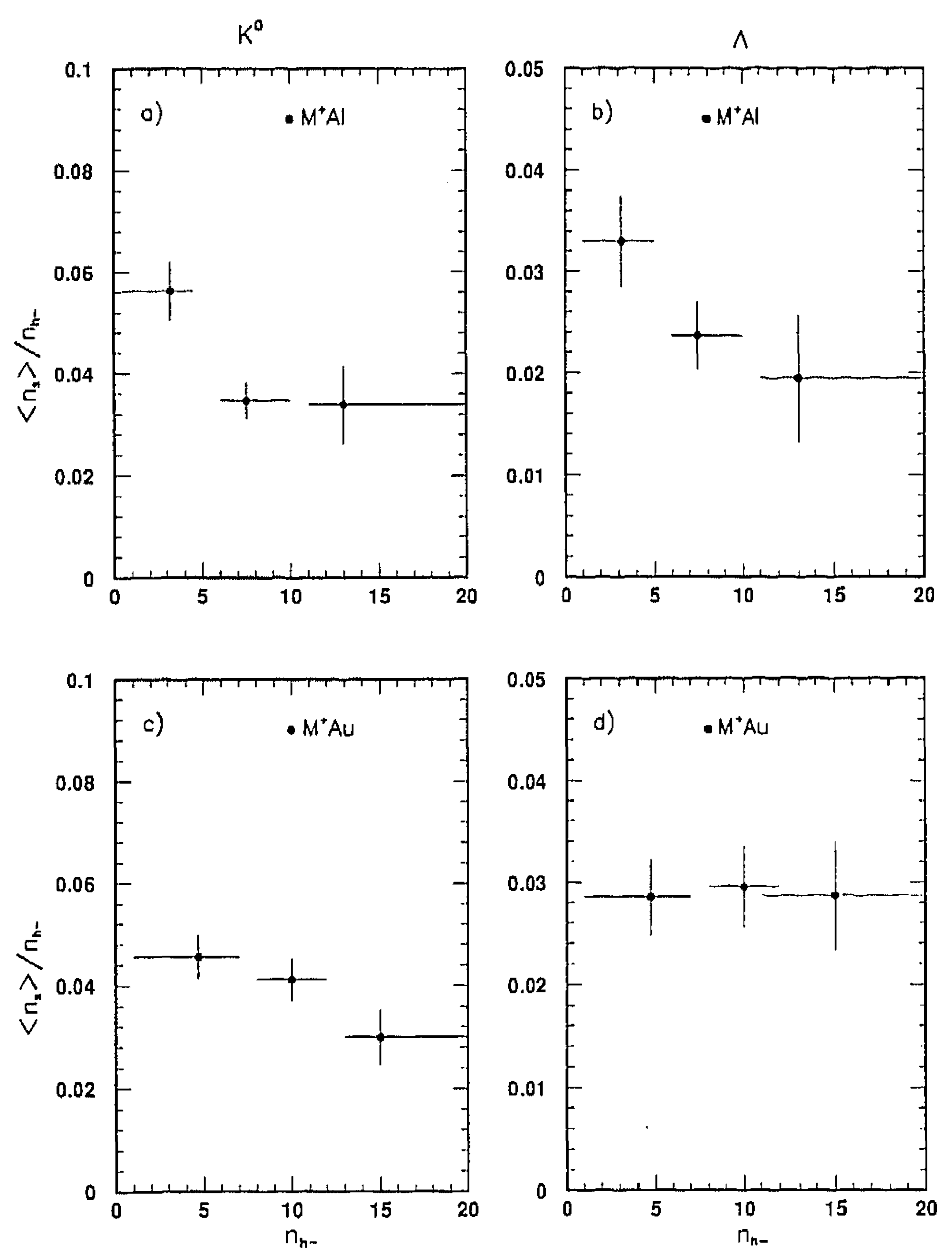


Fig. 11a-d. As in Fig. 10 but $\langle n_s \rangle / n_{h^-}$ is plotted versus n_{h^-}

sions, compared to ordinary matter as given e.g. by the number of negative hadrons n_{h^-} . The number n_p of ejected protons or the number n_{h^-} of negative hadrons can serve as a measure of the centrality of the collision.

Figure 10 shows the ratio $\langle n_s \rangle / \langle n_{h^-} \rangle$ (with $s = K_S^0$ in Fig. 10a, c and $s = \Lambda$ in Fig. 10b, d) as a function of n_p for events which contain a neutral strange particle. Figure 11 shows the ratio $\langle n_s \rangle / n_{h^-}$ versus n_{h^-} . Both figures demonstrate that the relative production rate of strange particles does not increase with increasing centrality of the collisions.

6 Summary

We present results on the inclusive production of K_S^0 and Λ in K^+ and π^+ interactions with Al and Au nuclei at 250 GeV/c. The main results can be summarized as follows.

- The inclusive K_S^0 and Λ production cross sections follow a dependence $\sigma \sim A^\alpha$, with $\alpha \simeq 0.9$.
- The Λ -hyperons are mainly produced in the target fragmentation and central regions.
- The p_T^2 and m_T distributions of the K_S^0 and Λ in the reactions (1-8) are well described by a single exponential form.
- The relative production rate of K_S^0 to π^- shows a strong dependence on x_F and p_T^2 , very similar to elementary collisions.
- The quark-parton FRITIOF model and in particular its modified version FRITIOF', is in reasonable agreement with the data.
- The average number of Λ 's is proportional to the number of projectile collisions, the average number of K_S^0 's does not follow this trend.

- Strangeness production happens preferentially in central collisions but the *relative* production rate of strange to non-strange matter does not increase with increasing centrality.

Acknowledgements. We are indebted to the CERN SPS, beam and EHS crews for their support during the preparation and runs of our experiment. It is a pleasure to thank the scanning and measuring staffs of our laboratories for their tedious effort in scanning and measuring these events. The contribution of the groups which participated in the earlier phase of this experiment is gratefully acknowledged.

References

1. S. Fredriksson, G. Eilam, G. Berlad, L. Bergström: Phys. Rep. 144 (1987) 188
2. A. Bamberger et al.: Z. Phys. C - Particles and Fields 43 (1989) 25; J. Bartke et al.: Z. Phys. C - Particles and Fields 48 (1990) 191
3. H. Bärwolff et al.: Z. Phys. C - Particles and Fields 37 (1988) 337
4. M. Adamus et al.: Z. Phys. C - Particles and Fields 32 (1986) 475
5. I.V. Ajinenko et al.: Z. Phys. C - Particles and Fields 42 (1989) 377
6. A.S. Carroll et al.: Phys. Lett. 80B (1979) 319
7. I.V. Ajinenko et al.: Z. Phys. C - Particles and Fields 44 (1990) 573
8. I.V. Ajinenko et al.: Z. Phys. C - Particles and Fields 46 (1990) 525
9. M. Aguilar-Benitez et al.: Phys. Lett. 170B (1986) 1
10. B. Andersson, G. Gustafson, B. Nilsson-Almqvist: Nucl. Phys. B281 (1987) 289
11. P. Seyboth et al.: Strangeness Production in Ultrarelativistic Ion-Nucleus Reactions Measured by the NA-35 Streamer Chamber Experiment. XXIV Int. Conf. on High Energy Physics Munich 1988 Abstract A287; R. Stock: Hadron Spectra and Correlations, parallel session review talk at the same conf. (1988)
12. I. Derado et al.: Z. Phys. C - Particles and Fields 50 (1991) 31
13. N.N. Nikolaev: Z. Phys. C - Particles and Fields 44 (1989) 645